Strong-Field Ionization of Linear Molecules by a Bichromatic Elliptically Polarized Laser Field with Coplanar Counterrotating or Corotating Components of Different Frequencies

IOP Conf. Series: Journal of Physics: Conf. Series **1206** (2019) 012003 doi:10.1088/1742-6596/1206/1/012003

Strong-Field Ionization of Linear Molecules by a Bichromatic Elliptically Polarized Laser Field with Coplanar Counterrotating or Corotating Components of Different Frequencies

A Gazibegović-Busuladžić[1], M Busuladžić[2], A Čerkić[1], E Hasović[1], W Becker[3,4] and D B Milošević[1,3,5]

1 Faculty of Science, University of Sarajevo, Sarajevo, Bosnia and Herzegovina
2 Faculty of Medicine, University of Sarajevo, Sarajevo, Bosnia and Herzegovina
3 Max-Born-Institut, Berlin, Germany
4 National Research Nuclear University (MEPhI), Moscow, Russia
5 Academy of Sciences and Arts of Bosnia and Herzegovina, Sarajevo, Bosnia and Herzegovina

E-mail: milo@bih.net.ba

Abstract. We investigate strong-field ionization of linear molecules by a two-color laser field of frequencies $r\omega$ and $s\omega$ having coplanar counterrotating or corotating elliptically polarized components (ω is the fundamental laser field frequency and r and s are integers). Using the improved molecular strong-field approximation we analyze direct above-threshold ionization (ATI) and high-order ATI (HATI) spectra. More precisely, reflection and rotational symmetries of these spectra for linear molecules aligned in the laser-field polarization plane are considered. The reflection symmetries for particular molecular orientations, known to be valid for a bicircular field (this is the field with circularly polarized counterrotating components), are valid also for arbitrary component ellipticities. However, specific rotational symmetries that are satisfied for HATI by a bicircular field, are violated for an arbitrary elliptically polarized field with counterrotating components. For the corotating case and the N_2 molecule we analyze molecular-orientation-dependent interferences and plateau structures for various ellipticities.

1. Introduction

Above-threshold ionization (ATI) is one of the most important nonlinear phenomena that may occur during the interaction of the strong laser field with atoms or molecules (see the review articles [1, 2, 3, 4] and references therein). In this process, the considered atomic or molecular system absorbs more photons from the laser field than is necessary for ionization. The electron, once liberated, goes directly to the detector. ATI can be the first step for some other more complicated phenomena. For example, due to the influence of the laser field, the ionized electron may return to the parent atomic or molecular ion (second step) and elastically scatter off it (third step), before reaching the detector. In this process, the electron can absorb many more photons from the laser field than in direct ATI. This process was named high-order ATI or HATI [1]. The electron energy spectra of the atomic or molecular HATI process are characterized by a plateau, that is, a broad energy range within which the photoelectron (HATI) yield is practically constant. The plateau is terminated by an abrupt cutoff after which the electron yield quickly drops by

orders of magnitude. Due to the more complicated structure of molecules, their (H)ATI spectra are much richer than those of atoms [5, 6, 7, 8, 9].

All cited papers are devoted to molecular HATI generated by a linearly polarized field. In this paper, we are interested in molecular (H)ATI by a bichromatic elliptically polarized laser field. Various nonlinear processes, including atomic and molecular HATI, generated by strong bichromatic elliptically polarized laser fields have attracted a lot of attention in the last few years. This is particularly true for the special case of a bichromatic elliptically polarized laser field that is called a bicircular field. This field consists of two coplanar corotating or counterrotating circularly polarized fields having different angular frequencies. A more detailed description of this type of laser field will be presented in the next section.

The (H)ATI process by a bicircular field was considered in [10], where a superposition of two counterrotating circularly polarized pulses, having the same frequency, was considered. One of these pulses was long while the other one was a few-cycle pulse. It was shown that high-energy electrons, generated in ionization by such a combination of pulses, are emitted in a direction correlated with the carrier-envelope phase of the few-cycle pulse. Angle-resolved electron energy spectra in strong-field ionization by a bicircular field of arbitrary frequencies $r\omega$ and $s\omega$ were analyzed in [11, 12]. For the ω–2ω case ($r = 1$ and $s = 2$), the predicted three-lobed shape of these spectra was recently confirmed experimentally [13]. Also, it was shown that the low-energy features of the photoelectron spectra are due to Coulomb-field-enhanced rescattering [13]. However, the high-energy features, also visible in the observed spectra presented in [13], were not explained. The high-energy spectra have recently been considered theoretically in [14, 15] and experimentally in [16]. In [17], the HATI spectra obtained in bicircular laser fields for different atomic targets are analyzed in detail using the quantum-orbit formalism. This approach gives more physical insight into the (H)ATI process. For this purpose, a specific classification of the saddle-point solutions was introduced both for the backward-scattered and for the forward-scattered electrons. The short forward-scattering quantum orbits for a bicircular field are similar to those of a linearly polarized field. The conclusion was that these orbits are universal, i.e., they do not depend on the shape of the laser field [17].

Very few papers have been devoted to molecular HATI generated by a bicircular laser field. In [18], we extended our theoretical approach from atomic HATI by a bicircular field to bicircular HATI from molecular targets. We considered the general symmetries of homonuclear molecules in a counterrotating bicircular laser field and identified four of them (two rotational and two reflection symmetries) that are satisfied in ATI of homonuclear diatomic molecules. It is important to stress that the two rotational symmetries are valid both for the direct ATI and for the rescattered electrons. All mentioned symmetries were illustrated using the N_2 molecule as the target and an ω–2ω bicircular laser field. The next step in our investigation was an analysis of the reflection and rotational symmetries for diatomic heteronuclear molecules and symmetric and asymmetric linear triatomic molecules [19]. It was shown that the (H)ATI spectra of symmetric linear molecules observe additional symmetries compared with the asymmetric case [19]. In [20] we have shown that, in contrast to atoms, the HATI spectra of nonlinear polyatomic molecules such as O_3 do not obey rotational symmetry in general. For the ω–2ω case, the HATI photoelectron momentum distribution has a three-lobed shape, as expected, but the rotational symmetry is absent. O_3 is a symmetric planar molecule and, for the ω–3ω bicircular field, the HATI spectrum is rotationally symmetric only if the plane of the molecule is perpendicular to the polarization plane of the laser field [20]. In [21] the authors have analyzed molecular ATI by polychromatic circularly polarized laser pulses. ATI spectra of the H_2^+ molecule are presented using solutions of the corresponding time-dependent Schrödinger equation. The results demonstrate the dependence of molecular photoionization on the frequency combination and helicity [21]. The influence of different laser and molecular parameters on the ATI spectra of the H_2^+ molecule was analyzed in [22]. Special attention was devoted to the sensitivity of

the corresponding spectra to the carrier-envelope phase. Molecular ATI minima and plateau structures as functions of the orientation of the considered molecule with respect to the major axis of the laser-field polarization ellipse were investigated in [23].

The main body of this paper is divided into three sections. In section 2 we define the transition matrix element, introduce our improved molecular strong-field approximation (MSFA) and define our bichromatic elliptically polarized field for both counterrotating and corotating components. In section 3 we present numerical results obtained using both the direct MSFA and the improved MSFA (IMSFA; [24] and references therein), which also takes into account rescattering. Finally, section 4 contains our concluding remarks and some discussion. The atomic system of units is used.

2. Notation and Theory

In our calculations we suppose that the laser field, the molecule, and the emitted electron all lie in the same plane (figure 1). We consider examples of homonuclear and heteronuclear diatomic as well as triatomic linear molecules. In our theoretical approach, a linear polyatomic molecule is modeled by an $(N+1)$-particle system, which consists of N heavy atomic (ionic) centers and one valence electron. After separation of the center of mass, we denote by $\mathbf{R} \equiv \{\mathbf{R}\} = (\mathbf{R}_1, \mathbf{R}_2, \ldots, \mathbf{R}_{N-1})$ the set of relative coordinates of all atomic centers. The vector $\mathbf{R}_N \equiv \mathbf{r}$ describes the relative motion of the electron with respect to the center of mass. More information about our notation can be found in [24].

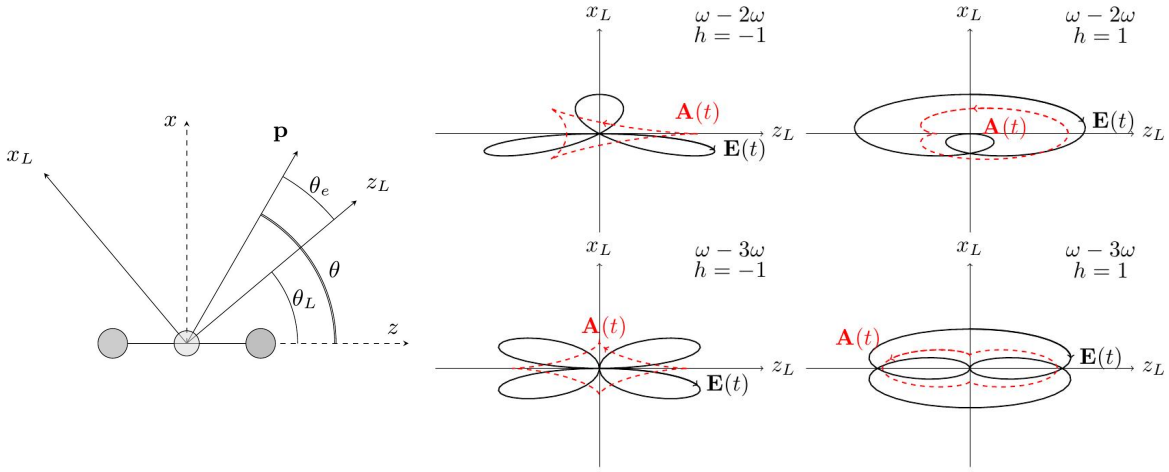

Figure 1. Left: Schematic presentation of the coordinate systems used in the paper. The linear molecule is along the z axis in the $0zxy$ coordinate system. The laser field lies in the $0z_Lx_L$ plane of the $0z_Lx_Ly_L$ coordinate system, which is rotated about the axis that is perpendicular to the $0zx$ plane ($y = y_L$ axis) by the angle θ_L with respect to the z axis. The direction of the electron momentum $\mathbf{p}$ is determined by the angle θ_e with respect to the z_L axis. The angles are positive for counterclockwise rotation (from z to x). Right: Electric-field vector $\mathbf{E}(t)$ (black solid curves) and vector potential $\mathbf{A}(t)$ (red dotted curves) of the bichromatic elliptically polarized field (2) for $r = 1$ and $s = 2$ (upper panels) and for $r = 1$ and $s = 3$ (bottom panels). The left-hand panels correspond to the counterrotating combination of the field components ($h = -1$), while those on the right-hand side are for corotating field components ($h = 1$). The component ellipticities are $\varepsilon_1 = \varepsilon_2 = \varepsilon = 0.3$.

For linear molecules all vectors of the set $\{\mathbf{R}\}$ are along the z axis. The laser field is defined in the coordinate system $\mathrm{O}z_Lx_L$, which is rotated with respect to the $\mathrm{O}zx$ system by the angle θ_L about the $y = y_L$ axis, which is perpendicular to the polarization plane. The momentum $\mathbf{p}$

of the emitted electron is determined by the angles θ_e in the Oz_Lx_L system and $\theta = \theta_L + \theta_e$ in the Ozx system. The unit vectors of the corresponding coordinate systems are related by

$$\hat{\mathbf{e}}_{\rm Lz} = \hat{\mathbf{z}}\cos\theta_L + \hat{\mathbf{x}}\sin\theta_L,\ \hat{\mathbf{e}}_{\rm Lx} = -\hat{\mathbf{z}}\sin\theta_L + \hat{\mathbf{x}}\cos\theta_L. \tag{1}$$

We consider a bichromatic elliptically polarized field having the period T and the fundamental frequency $\omega = 2\pi/T$, with the electric-field vector [25]

$$\mathbf{E}(t) = \frac{E_1}{\sqrt{1+\varepsilon_1^2}}[\hat{\mathbf{e}}_{\rm Lz}\sin(r\omega t) - \hat{\mathbf{e}}_{\rm Lx}\varepsilon_1\cos(r\omega t)] + \frac{E_2}{\sqrt{1+\varepsilon_2^2}}[\hat{\mathbf{e}}_{\rm Lz}\sin(s\omega t+\phi) - h\hat{\mathbf{e}}_{\rm Lx}\varepsilon_2\cos(s\omega t+\phi)]. \tag{2}$$

We assume equal component strengths and fix the relative phases to zero ($E_1 = E_2 = E_L$, $\phi = \phi_1 = \phi_2 = 0$ compared with the notation of [17]). In figure 1 we present parametric plots of the ω–2ω and ω–3ω counterrotating ($h = -1$) and corotating ($h = +1$) bichromatic elliptically polarized fields as well as the corresponding vector potentials. The ellipticities of the laser-field components are the same ($\varepsilon_1 = \varepsilon_2 = \varepsilon = 0.3$).

Inspection of the Lissajous figures of the fields (2) and the corresponding vector potentials shown in Fig. 1 suggests already that one should not expect the rotational and reflection symmetries of the electron velocity maps that exist for circularly polarized field components. At best, in the ω–2ω case, one reflection symmetry might be expected to survive for suitable molecular orientations and no rotational symmetry. The threefold symmetry of the velocity maps, which is so typical of ATI spectra of bicircular fields, will be destroyed as soon as the component fields are no longer circular. In the ω–3ω case, one might expect to observe inversion symmetry in special cases, certainly not the fourfold rotational symmetry of the bicircular case. The details require a detailed investigation, which we will present in the remainder of this paper.

We use the improved molecular strong-field approximation ([24] and references therein) to calculate the differential ionization rate for emission of an electron with the final momentum $\mathbf{p}$:

$$w_{\mathbf{R}\mathbf{p}i}(n) = 2\pi p\,|T_{\mathbf{R}\mathbf{p}i}(n)|^2\,. \tag{3}$$

Here $n = n_1 r + n_2 s$, and n_1 photons of frequency $r\omega$ and n_2 photons of frequency $s\omega$ are absorbed from the two-color elliptically polarized field (2). In the IMSFA the T-matrix element of the (H)ATI process can be written as

$$T_{\mathbf{R}\mathbf{p}i}(n) = \int_0^T \frac{dt}{T}\left[\mathcal{F}^{(0)}_{\mathbf{R}\mathbf{p}i}(t) + \mathcal{F}^{(1)}_{\mathbf{R}\mathbf{p}i}(t)\right] e^{in\omega t + i\mathcal{U}(t)}, \tag{4}$$

with the time-periodic functions $\mathcal{F}^{(j)}_{\mathbf{R}\mathbf{p}i}(t)$, $j = 0, 1$, and $\mathcal{U}(t) = \mathbf{p}\cdot\boldsymbol{\alpha}(t) + \int^t d\tau\mathbf{A}^2(\tau)/2 - U_{\rm p}t$, where $\boldsymbol{\alpha}(t) = \int^t d\tau\mathbf{A}(\tau)$, $U_{\rm p}$ is the ponderomotive energy, and $\mathbf{A}(t) = -\int^t d\tau\mathbf{E}(\tau)$. The energy-conservation condition has the form $E_{\mathbf{p}} = \mathbf{p}^2/2 = n\omega - I_{\rm p} - U_{\rm p}$. For asymmetric molecules, the unperturbed ionization potential $I_{\rm p}$ should be replaced by $I_{\rm p} - \Delta_S$, where Δ_S is the polarizability-induced Stark shift [26]. For our bicircular field, we have $\Delta_S = -E_L^2(\alpha_\parallel + \alpha_\perp)/4$, where $\alpha_\parallel$ and $\alpha_\perp$, respectively, are the polarizability parallel and perpendicular to the molecular axis.

The zeroth-order term, which corresponds to the direct ATI electrons, for neutral polyatomic molecules is described by the matrix element [24]

$$\mathcal{F}^{(0)}_{\mathbf{R}\mathbf{p}i}(t) = \sum_{j=1}^{N} f(\boldsymbol{\rho}_j, t)e^{-i\mathbf{p}\cdot\boldsymbol{\rho}_j}\sum_a c_{ja}\langle\mathbf{p} + \mathbf{A}(t)|\mathbf{E}(t)\cdot\mathbf{r}|\psi_a\rangle, \tag{5}$$

where the c_{ja} are the coefficients of an expansion of the molecular electronic ground-state wave function in a linear combination of the atomic orbitals ψ_a. For symmetric linear molecules and

dressed atomic orbitals, we have $f(\boldsymbol{\rho}_j, t) = 1$, while for asymmetric linear molecules and dressing of the whole molecular orbital we have $f(\boldsymbol{\rho}_j, t) = \exp\{i[\mu_S(t) + \alpha_S(t) - \mathbf{A}(t) \cdot \boldsymbol{\rho}_j]\}$. The two time-dependent terms, $\mu_S(t) = \int^t \boldsymbol{\mu} \cdot \mathbf{E}(t')dt'$ and $\alpha_S(t) = \int^t \left[\alpha_\parallel E_\parallel^2(t') + \alpha_\perp E_\perp^2(t')\right] dt'/2 + \Delta_S t$, enrich the oscillatory structure of the spectra. Here $\boldsymbol{\mu} = -\mu\hat{\mathbf{z}}$ is the electric dipole vector and $E_\parallel(t)$ $[E_\perp(t)]$ is the electric-field vector parallel (perpendicular) to the molecular axis. The coordinates $\boldsymbol{\rho}_j$ are defined in [24] as linear combinations of the relative coordinates $\{\mathbf{R}\}$. For $N = 2$, we have $\boldsymbol{\rho}_j = -(q - \lambda)\mathbf{R}_1/2$, where $\lambda = (m_1 - m_2)/(m_1 + m_2)$ is the mass asymmetry parameter and $q = +1$ for $j = 1$ and $q = -1$ for $j = 2$. In this case, the sum over j in equation (5) is replaced by the sum over $q = \pm 1$. For $\lambda = 0$, this reduces to the result known for homonuclear diatomic molecules from [27].

The first-order term, which corresponds to the rescattered electrons, for neutral polyatomic molecules has the form

$$\begin{aligned}\mathcal{F}^{(1)}_{\mathbf{Rp}i}(t) &= -ie^{-iS_{\mathbf{k}_{\rm st}}(t)} \int_0^\infty d\tau \left(\frac{2\pi}{i\tau}\right)^{3/2} e^{i\left[S_{\mathbf{k}_{\rm st}}(t') - (I_{\rm p} - \Delta_S)\tau\right]} \\ &\times \sum_{j=1}^{N} e^{i\mathbf{K}\cdot\boldsymbol{\rho}_j} V^j_{e\mathbf{K}} \sum_{l=1}^{N} f(\boldsymbol{\rho}_l, t') e^{-i\mathbf{k}_{\rm st}\cdot\boldsymbol{\rho}_l} \sum_a c_{la} \langle \mathbf{k}_{\rm st} + \mathbf{A}(t')|\mathbf{E}(t') \cdot \mathbf{r}|\psi_a\rangle, \end{aligned} \tag{6}$$

with $t' = t - \tau$, $\mathbf{K} = \mathbf{k}_{\rm st} - \mathbf{p}$, $\mathbf{k}_{\rm st} = \int_t^{t'} dt'' \mathbf{A}(t'')/\tau$ the stationary electron momentum, and $S_{\mathbf{k}}(t) = \int^t dt'[\mathbf{k} + \mathbf{A}(t')]^2/2$. In the above equation, $V^j_{e\mathbf{K}}$ is the Fourier transform of the rescattering potential at the jth atomic (ionic) center.

3. Numerical results

In this section we will show our numerical results obtained using the MSFA (for direct ATI) and the IMSFA (both the direct ATI and the rescattered HATI electrons are included) introduced in section 2. We will show the photoelectron momentum distributions in the $p_z p_x$ plane using a false-color presentation with a logarithmic scale that covers six orders of magnitude. The electron-momentum plane is defined with respect to the laser-field coordinate system: $p_z = p\cos\theta_e$, $p_x = p\sin\theta_e$. The value of the angle θ_L between the z axis, which is along the internuclear axis, and the major axis of the laser-field polarization ellipse is fixed. Unless stated otherwise, the results are presented for the photoelectron kinetic energies $E_{\mathbf{p}} \leq 12U_{\rm p}$. We will refer to these distributions as the (H)ATI spectra although the photoelectron energy spectra are presented only in the right-hand subpanels of figure 5.

In the first part of this section, numerical results will be presented calculated for the case of counterrotating field components. In our previous papers [18, 19] we have analyzed in detail the symmetries of the corresponding (H)ATI spectra for various molecular species, for the special case of a bicircular field. In this case, the value of the ellipticity is $\varepsilon = 1$ and the field components are counterrotating. Here, we are going to consider symmetries for (H)ATI spectra generated by a counterrotating field when $|\varepsilon| < 1$. More precisely, our aim is to analyze the reflection symmetries of the corresponding ATI spectra and the rotational symmetries of the corresponding HATI spectra. Results for the molecules N_2, CO, and CO_2 will be presented.

In the second part of this section we will display our numerical results for the corotating bichromatic elliptically polarized laser field. The N_2 molecule is used as a target. We analyze the (H)ATI spectra for different molecular orientations and combinations of the angular frequencies of the field components. The length and the height of the rescattering plateau will be analyzed as a function of the molecular orientation.

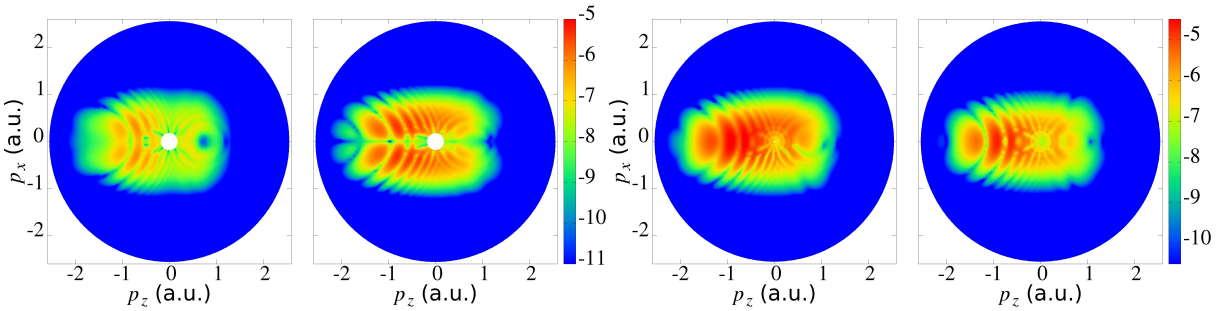

Figure 2. The figures in the two left-hand panels correspond to the ATI spectra for the CO_2 molecule obtained using our MSFA. The first panel is for $\theta_L = 0°$ and the second for $\theta_L = 90°$. The two panels on the right-hand side exhibit the ATI spectra for the CO molecule; the first panel is for $\theta_L = 0°$ and the second for $\theta_L = 90°$. The intensities of the ω–2ω counterrotating laser-field components are 10^{14} W/cm^2, the ellipticities are $\varepsilon_1 = \varepsilon_2 = \varepsilon = 0.3$, and the fundamental wavelength is 800 nm.

3.1. Counterrotating case

First, we consider reflection symmetries for the direct (ATI) photoelectron spectra in a bichromatic counterrotating elliptically polarized field. For the analysis of reflection symmetries we consider ATI spectra for the CO_2 molecule, which is taken as an example of the symmetric linear molecule, and for the CO molecule, which is a heteronuclear diatomic molecule (and hence an example of the asymmetric case). Spectra for two molecular orientations, $\theta_L = 0°$ and $\theta_L = 90°$, are considered. In [19] we have shown that the ATI spectra of linear symmetric molecules in a bicircular counterrotating field exhibit reflection symmetries for the molecular orientations $\theta_L = 0°$ and $\theta_L = 90°$. Also, in [19] it was shown that, for the ATI spectra of asymmetric linear molecules in a bicircular counterrotating field, there are no reflection symmetries for the molecular orientation $\theta_L = 0°$. In general, the reason for reflection symmetry to appear in the ATI spectra is the invariance with respect to the transformation $x \to -x$, $\mathbf{A}(t) \to \mathbf{A}(-t)$, $\mathbf{E}(t) \to -\mathbf{E}(-t)$. This also holds in the case of a bichromatic elliptically polarized field $|\varepsilon| < 1$. So, as shown in the first and the second panels of figure 2, the same reflection symmetry is present in the ATI spectra for $\varepsilon = 0.3$ and the symmetric CO_2 molecule. The third panel from the left in figure 2 corresponds to the asymmetric CO molecule oriented along the z_L axis ($\theta_L = 0°$). It is clear that, as opposed to the other cases presented in figure 2, there is no reflection symmetry in this case.

Let us now consider the rotational symmetries of the HATI spectra. For a bicircular field it was shown that the spectra exhibit invariance with respect to rotation by the dynamical-symmetry angle $\alpha_j = -2\pi jr/(r+s)$ (j integer) of the bicircular field. The mentioned dynamical symmetry is given by the relation $R_y(\alpha_j)\mathbf{E}(t) = \mathbf{E}(t+\tau_j)$, where $R_y(\alpha_j)$ is the 2×2 rotation matrix representing the rotation by the angle α_j about the y axis, and $\tau_j = jT/(r+s)$. As the consequence, the following symmetry transformation is valid: $\theta_L \to \theta_L - \alpha_j$, $\quad \theta_e \to \theta_e + \alpha_j$ (this means that the spectra are invariant with respect to this transformation). However, for $|\varepsilon| < 1$ this dynamical symmetry is violated, and the corresponding rotational invariance is absent. This can be seen both in the right-hand-side pair of the panels and in the left-hand-side pair of the panels of figure 3. In contrast to the bicircular-field case, the invariance with respect to the transformation $\theta_L \to \theta_L + 120°$, $\theta_e \to \theta_e + 120°$ is violated.

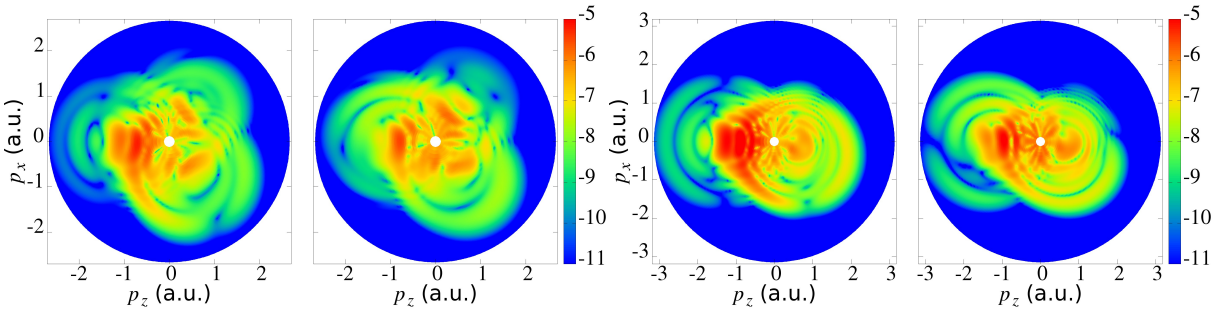

Figure 3. HATI spectra, obtained using our IMSFA, for ionization of the N_2 molecule by an elliptically polarized counterrotating ω–2ω laser field with component intensities 10^{14} W/cm^2 and the fundamental wavelength 800 nm. For the two left-hand panels the ellipticity is $\varepsilon = 0.8$ and the spectra are calculated for $E_{\mathbf{p}} \leq 12U_{\mathrm{p}}$, while for the two right-hand panels we have $\varepsilon = 0.3$ and $E_{\mathbf{p}} \leq 17U_{\mathrm{p}}$. In both cases the first panel is for $\theta_L = 0°$ and the second one is for $\theta_L = 120°$.

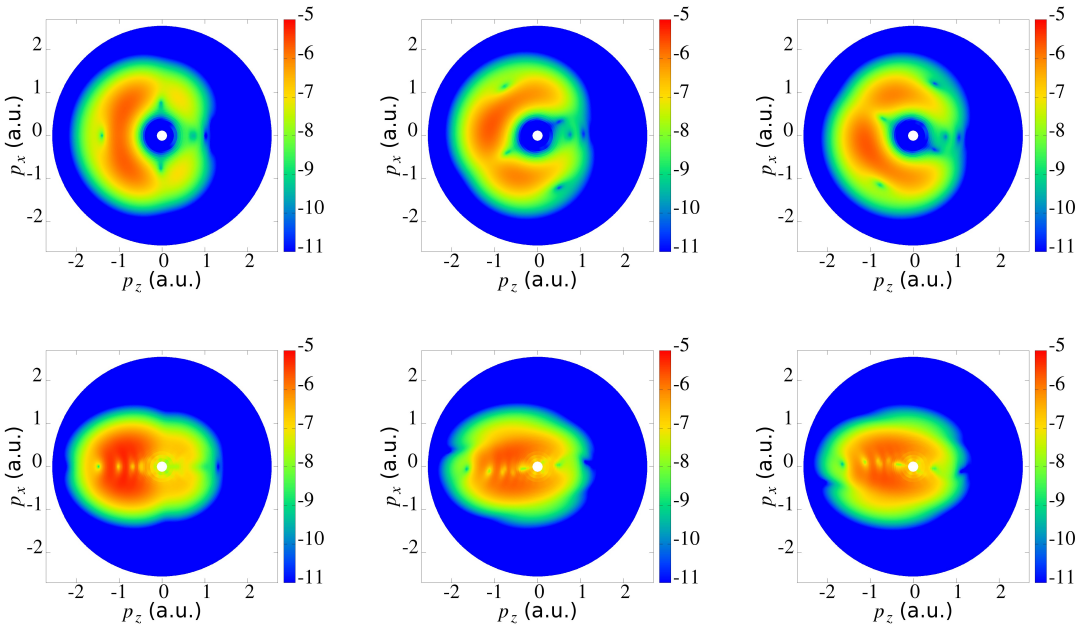

Figure 4. Direct ATI photoelectron spectra obtained using the MSFA for the N_2 molecule and corotating fields. The laser field intensity is 10^{14} W/cm^2 and the fundamental wavelength of the laser field is 800 nm. The combination of the angular frequencies of the corotating field components is ω–2ω. The angle between the z axis, which is along the internuclear axis, and the major axis of the laser-field polarization ellipse is $\theta_L = 0°$ (left panels, parallel orientation), $\theta_L = 60°$ (middle panels), and $\theta_L = 120°$ (right panels). The ellipticities of the laser field are $\varepsilon = 1$ (upper panels) and $\varepsilon = 0.3$ (lower panels).

3.2. Corotating case

In this subsection we present our numerical results for a corotating bichromatic elliptically polarized laser field. The N_2 molecule is used as a target. We first analyze the spectra of direct electrons for various ellipticities and molecular orientations. It is again assumed that the

ellipticities and intensities of the two field components are equal ($\varepsilon_1 = \varepsilon_2 = \varepsilon$ and $I_1 = I_2 = I$). In figure 4, the logarithm of the differential ionization rate of the N_2 molecule is presented in false colors in the electron momentum plane for direct ATI by a bichromatic elliptically polarized ω–2ω laser field having the component intensities 10^{14} W/cm^2 and the fundamental wavelength 800 nm. The angle of molecular orientation is $\theta_L = 0^\circ$ (left panels), $\theta_L = 60^\circ$ (middle panels), and $\theta_L = 120^\circ$ (right panels). The spectra shown in the upper and lower panels of figure 4 are calculated for $\varepsilon = 1$ and $\varepsilon = 0.3$, respectively.

All spectra presented in figure 4 are characterized by two-center destructive interference minima. One of them is clearly visible for $\theta_e = 180^\circ$ and $p_z \approx -1.5$ a.u. in the upper left panel of figure 4. By performing a detailed analysis, we confirmed that these minima are due to the interference of wave packets emitted from the two molecular centers [23]. Namely, comparing the integrated differential ionization rate and the partial contributions that include only ionization from one of the molecular centers, one can determine the origin of the above-mentioned minima. Taking into account the molecular symmetry, as well as the atomic orbitals that make up the highest occupied molecular orbital (HOMO) of the considered molecule, we are able to find conditions that allow one to determine the positions of the two-center destructive-interference minima. More precisely, the connection between the coefficients c_{sa} appearing in the linear combination of atomic orbitals [27] depends on the symmetry of the considered molecule and is given by $c_{-1a} = s_{a\lambda} c_{1a}$, with

$$s_{a\lambda} = (-1)^{l_a - m_a} \begin{cases} (-1)^{m_\lambda} & \text{(for g-symmetry)} \\ (-1)^{m_\lambda + 1} & \text{(for u-symmetry)} \end{cases} . \tag{7}$$

Here, m_λ is the projection of the orbital angular momentum on the internuclear axis. For example, for $3\sigma_g$ states it is $m_\lambda = 0$. The factor $(-1)^{l_a - m_a}$ comes from the inversion of the z coordinate of the second center. It can be shown that the observed minima are determined by the following expressions [23]

$$p^{(+1)}_{\mathrm{min},m} = \frac{(2m+1)\pi}{R\cos(\theta_e - \theta_L)}, \quad p^{(-1)}_{\mathrm{min},m} = \frac{2(m+1)\pi}{R\cos(\theta_e - \theta_L)}, \tag{8}$$

where $m = 0, 1, 2, \ldots$. For the used laser and molecular parameters the minima that correspond to $p^{(+1)}_{\mathrm{min},0}$ and $p^{(-1)}_{\mathrm{min},-1}$ are clearly visible in the upper left panel of figure 4. If we take into account only the orbitals with l_a even, the interference minima form a straight line $p_z = -\pi/R$ in the momentum plane, while for l_a odd we have $p_z = 0$. Since both even and odd orbitals contribute to the spectra, the mentioned minima are partially masked, as can be seen in the upper left panel of figure 4 ($\theta_L = 0^\circ$). Comparing this result with those presented in the other upper panels, we see that the positions of the minima are rotated by the angle $-\theta_L$, which is in accordance with equation (8). For example, for the upper right panel ($\theta_L = 120^\circ$) the minimum appears for $\theta_e = 60^\circ$. The spectra for parallel orientation (and also for perpendicular orientation; see figure 3 in [23]) obey reflection symmetry with respect to the p_z axis. This is clearly visible for $\theta_L = 0^\circ$ in the left panels of figure 4. For any other orientation this type of symmetry is broken. Comparing the corresponding middle and right panels of figure 4 we see that the spectra are invariant with respect to the transformation: $\theta_L \to 180^\circ - \theta_L$, $p_x \to -p_x$. For $\varepsilon = 0.3$, a series of minima can be observed along the z axis. These minima are caused by the interference of the parts of the wave packets emitted from the same center of the N_2 molecule [23].

Now, we focus on the difference between the yield of high-energy photoelectrons emitted nearly antiparallel to the major axis of the laser-field polarization ellipse for perpendicular and for parallel molecular orientation. It can be shown that the corresponding yield for $\theta_e = 180^\circ$ and perpendicular orientation is one order of magnitude higher than that for parallel orientation [23]. This effect exists for a wide range of laser field intensities, ellipticities, and wavelengths.

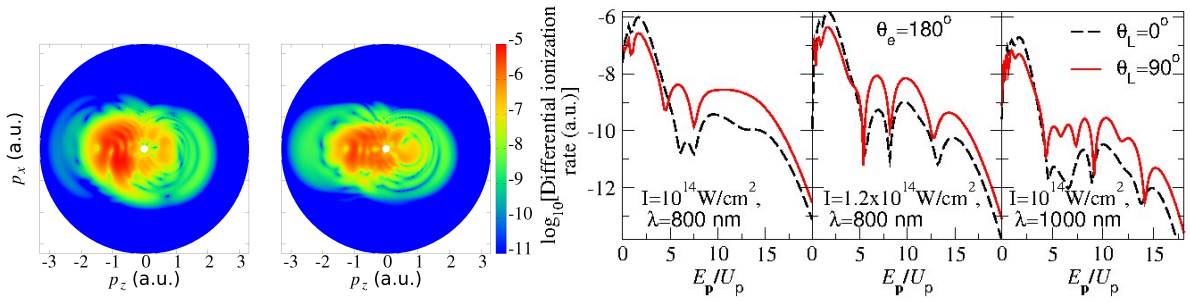

Figure 5. HATI photoelectron spectra obtained using the IMSFA for the N_2 molecule in a bichromatic ω–2ω corotating field with the ellipticity $\varepsilon = 0.3$. Left two subpanels: the molecular orientation angle is $\theta_L = 0°$ (left) and $\theta_L = 90°$ (right), the field component intensities are $I = 10^{14}$ W/cm^2 and the fundamental wavelength is $\lambda = 800$ nm. The results are presented for $E_\mathbf{p} \leq 18U_\mathrm{p}$. The right three subpanels: the logarithm of the differential ionization rate in atomic units is presented as a function of the photoelectron kinetic energy in units of the ponderomotive energy for the laser parameters given in each subpanel [$I = 10^{14}$ W/cm^2, $\lambda = 800$ nm (left), $I = 1.2 \times 10^{14}$ W/cm^2, $\lambda = 800$ nm (middle), and $I = 10^{14}$ W/cm^2, $\lambda = 1000$ nm (right)].

It is clearly visible in the plots presented in the three right-hand subpanels of figure 5. These plots exhibit the plateau height for two different intensities and wavelengths for the orientations $\theta_L = 0°$ and $\theta_L = 90°$ of the N_2 molecule, the emission angle $\theta_e = 180°$, and for the elliptically polarized corotating ω–2ω field with $\varepsilon = 0.3$.

In the two left subpanels of figure 5 we show the complete photoelectron momentum distributions for the same laser parameters as used in the first (left) of the three right subpanels of figure 5. Analyzing these spectra we conclude that they confirm our general conclusion that the reflection and rotational symmetries are violated for HATI spectra if $|\varepsilon| < 1$ and $r + s$ odd. Also, it is clearly visible that long plateaus are well developed for high electron energies for $\varepsilon = 0.3$ and $\theta_L = 0°$ and $\theta_L = 90°$. We have checked that this is valid for all molecular orientations for the corotating field if $|\varepsilon| < 0.5$.

In our previous investigation [23] we have shown that for $r = 1$ and $s = 2$ the plateau for $\theta_e = 180°$ is longer than that for $\theta_e = 0°$. On the other hand, for the case $r = 1$ and $s = 3$ the plateau for $\theta_e = 180°$ is of the same length and height as the plateau for $\theta_e = 0°$. The reason is the actual symmetry that the HATI spectra for symmetric molecules obey, if exposed to a corotating elliptically polarized laser field with $r+s$ even. Namely, for symmetric molecules and for $r + s$ even we have invariance with respect to the transformation

$$\theta \to \theta + j180°,\ \theta_L \to \theta_L,\ \theta_e \to \theta_e + j180°,\ (r + s = \text{even}, j \text{ integer}) \tag{9}$$

which corresponds to the transformation $\mathbf{p} \to -\mathbf{p}$ with fixed positions of the molecule and the field. This *inversion symmetry* is clearly visible in all three panels of figure 6.

4. Conclusions

Using the improved molecular strong-field approximation, we investigated the strong-field ionization of the oriented linear molecules N_2, CO, and CO_2 by counterrotating and corotating bichromatic elliptically polarized laser fields. The photoelectron spectra of both the direct (ATI) and the rescattered (HATI) electrons were analyzed.

For symmetric molecules and counterrotating fields the direct ATI spectra obey reflection symmetry about the p_z axis in the laser-field coordinate system for both parallel and perpendicular molecular orientations. In the case of asymmetric molecules this is valid only

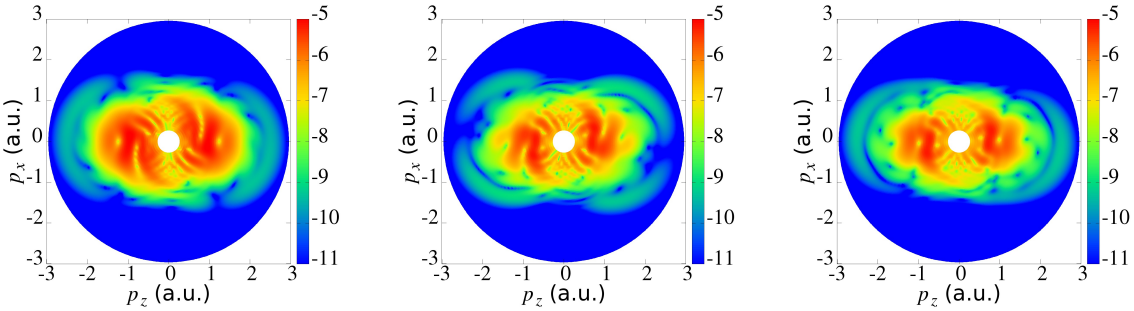

Figure 6. Photoelectron HATI spectra obtained using the IMSFA for the N_2 molecule and fixed value of the ellipticity $\varepsilon_1 = \varepsilon_2 = \varepsilon = 0.3$. The three presented momentum distributions correspond to different values of the molecular orientations: $\theta_L = 0°$, $\theta_L = 60°$, and $\theta_L = 90°$, from left to right, respectively. The intensities of the ω–3ω corotating laser-field components are 10^{14} W/cm^2 and the fundamental wavelength is 800 nm. Results are presented for $E_{\mathbf{p}} \leq 17U_{\mathrm{p}}$.

for perpendicular molecular orientations. For other orientations, this symmetry is violated. These facts were known to be valid for a bicircular field ($\varepsilon = 1$) [18, 19] but we have now confirmed that they are satisfied for arbitrary ellipticity ε. In addition, we have found that for symmetric molecules the transformation $\theta_L \to 180° - \theta_L$ leads to $p_x \to -p_x$ in the ATI spectra.

Reflection symmetry is violated by the HATI spectra. For the counterrotating case the rotational symmetry ($\theta_L \to \theta_L - \alpha_j$, $\theta_e \to \theta_e + \alpha_j$), which is valid for HATI spectra when $\varepsilon = 1$, is no longer valid if $\varepsilon < 1$.

For a corotating bichromatic elliptically polarized laser field with ellipticity $\varepsilon < 0.5$ the high-energy plateau in the photoelectron spectra is well developed. In the ω–2ω case the high-energy plateau for $\theta_e = 180°$ is longer than the plateau for $\theta_e = 0°$. For the molecular orientation $\theta_L = 90°$ the plateau for $\theta_e = 180°$ is higher by one order of magnitude than for $\theta_L = 0°$. For symmetric molecules, in the ω–3ω case the high-energy plateau for $\theta_e = 180°$ is the same as that for $\theta_e = 0°$. The reason is that, for $r + s$ even and for symmetric molecules, the HATI spectra exhibit inversion symmetry, i.e. invariance with respect to the substitution $\mathbf{p} \to -\mathbf{p}$.

Underlying our results were equal ellipticities of the two component fields. In the most general case of unequal ellipticities it still remains to explore if some symmetries survive. We employed the (improved) molecular strong-field approximation whose reliability, in general, is not well known (for example, the Coulomb effects are not included). However, we expect that the symmetry properties of the velocity maps predicted by the (I)MSFA should be reliable and agree with solutions of the time-dependent Schrödinger equation. Hence, inspecting the symmetries of measured velocity maps and comparing them with the (I)MSFA predictions may provide valuable tools to determine, for example, deviations from perfect agreement of the actual fields from their desired form.

Acknowledgments

This work was supported in part by the Alexander von Humboldt Foundation.

References

[1] Becker W, Grasbon F, Kopold R, Milošević D B, Paulus G G and Walther H 2002 *Adv. At. Mol. Opt. Phys.* **48** 35
[2] Becker A and Faisal F H M 2005 *J. Phys.* B **38** R1
[3] Lein M 2007 *J. Phys.* B **40** R135
[4] Agostini P and DiMauro L F 2012 *Adv. At. Mol. Opt. Phys.* **61** 117

[5] Muth-Böhm J, Becker A and Faisal F H M 2000 *Phys. Rev. Lett.* **85** 2280
[6] Grasbon F, Paulus G G, Chin S L, Walther H, Muth-Böhm J, Becker A and Faisal F H M 2001 *Phys. Rev.* A **63** 041402(R)
[7] Dura J, Grün A, Bates P K, Teichmann S M, Ergler T, Senftleben A, Pflüger T, Schröter C D, Moshammer R, Ullrich J, Jaroń-Becker A, Becker A and Biegert J 2012 *J. Phys. Chem.* A **116** 2662
[8] Hetzheim H, Figueira de Morisson Faria C and Becker W 2007 *Phys. Rev.* A **76** 023418
[9] Suárez N, Chacón A, Pisanty E, Ortmann L, Landsman A S, Picón A, Biegert J, Lewenstein M and Ciappina M F 2018 *Phys. Rev.* A **97** 033415
[10] Hasović E, Milošević D B and Becker W 2006 *Laser Phys. Lett.* **3** 200
[11] Kramo A, Hasović E, Milošević D B and Becker W 2007 *Laser Phys. Lett.* **4** 279
[12] Hasović E, Kramo A and Milošević D B 2008 *Eur. Phys. J. Special Topics* **160** 205
[13] Mancuso C A, Hickstein D D, Grychtol P, Knut R, Kfir O, Tong X M, Dollar F, Zusin D, Gopalakrishnan M, Gentry C, Turgut E, Ellis J L, Chen M C, Fleischer A, Cohen O, Kapteyn H C and Murnane M M 2015 *Phys. Rev. A* **91** 031402(R)
[14] Hasović E, Becker W and Milošević D B 2016 *Opt. Express* **24** 6413
[15] Hoang V H, Le V H, Lin C D and Le A T 2017 *Phys. Rev. A* **95** 033402(R)
[16] Mancuso C A, Hickstein D D, Dorney K M, Ellis J L, Hasović E, Knut R, Grychtol P, Gentry C, Gopalakrishnan M, Zusin D, Dollar F J, Tong X M, Milošević D B, Becker W, Kapteyn H C, and Murnane M M 2016 *Phys. Rev. A* **93** 053406
[17] Milošević D B and Becker W 2016 *Phys. Rev. A* **93** 063418
[18] Busuladžić M, Gazibegović-Busuladžić A and Milošević D B 2017 *Phys. Rev. A* **95** 033411
[19] Gazibegović-Busuladžić A, Busuladžić M, Hasović E, Becker W and Milošević D B 2018 *Phys. Rev. A* **97** 043432
[20] Habibović D, Čerkić A, Busuladžić M, Gazibegović-Busuladžić A, Odžak S, Hasović E and Milošević D B 2018 *Opt. Quant. Electron.* **50** 214
[21] Yuan K J and Bandrauk A D 2018 *Phys. Rev. A* **98** 023413
[22] Abu-samha M and Madsen L B 2018 *J. Phys.* B **51** 135401
[23] Busuladžić M, Čerkić A, Gazibegović-Busuladžić A, Hasović E and Milošević D B 2018 *Phys. Rev. A* **98** 013413
[24] Hasović E and Milošević D B 2014 *Phys. Rev. A* **89** 053401
[25] Čerkić A, Busuladžić M, and Milošević D B 2017 *Phys. Rev. A* **95** 063401
[26] Hasović E, Busuladžić M, Becker W, and Milošević D B 2011 *Phys. Rev. A* **84** 063418
[27] Milošević D B 2006 *Phys. Rev. A* **74** 063404